

SPATIAL FILTRATION OF SHEAR INTERFEROGRAMS IN HOLOGRAPHIC INTERFEROMETRY OF A FOCUSED IMAGE

V.G. Gusev

*V.V. Kuibyshev State University, Tomsk
Received October 12, 1990*

An analysis is presented of a shear interferometer based on double-exposure recording of holograms of the focused image of a mat screen with two successive Fourier transforms. It is shown both theoretically and experimentally that spatial filtration in the hologram plane enables control of the field of a lens or an objective. The spatial filtering in the far diffraction zone makes it possible to record the interference pattern characterizing the phase distortions introduced in the wave illuminating the mat screen by the aberrations of the illuminating optical system.

An analysis of a technique for obtaining shear interferograms based on double-exposure recording of holograms of the focused image of a mat screen with spatial filtration of the diffusely scattered radiation field was carried out in Refs. 1 and 2. In these studies the construction of the image of the mat screen in the plane of the photographic plate was considered both for the case of two successive Fresnel transforms of the scattered radiation field and for the case of two successive Fourier transforms.

The optical scheme of image formation by coherent light is well known³⁻⁴ and, in particular, provides conditions under which the frequency transfer functions of a lens or an objective will be constant up to a certain maximum spatial frequency.

This paper considers some salient features of differential holographic interferometry with the help of such an optical scheme of image formation.

As is shown in Fig. 1 a mat screen positioned in the (x_1, y_1) plane is illuminated by a converging quasiperiodic wave. The radius of curvature of the wavefront is equal to the distance between the screen and the node of the lens L_1 . With the help of this lens an image of the mat screen is constructed in the plane (x_3, y_3) of the photographic plate 2. A hologram of the focused image is produced during the first exposure by an off-axis reference plane wave 3. It is assumed that prior to the second exposure the mat screen is displaced along the x axis by a distance a , while the lens L_1 is displaced along the same direction in its principal plane (x_2, y_2) by a distance b .

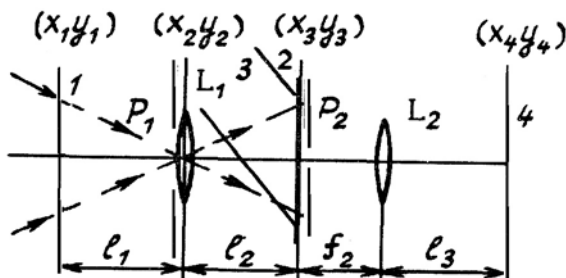


FIG. 1. Optical diagram of recording and reconstruction of the double exposure hologram of a focused image: 1) mat screen; 2) photographic plate hologram; 3) reference beam; 4) interferogram recording plane; L_1 and L_2 are lenses; p_1 and p_2 are diaphragms.

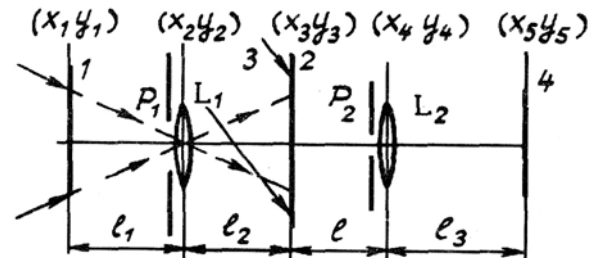


FIG. 2. Optical diagram of recording and reconstruction of the doubly exposed holograms in the case in which the image is localized outside the photographic plate.

We shall represent the distributions of the complex amplitudes of the fields from the first and second exposures in the plane of the photographic plate in the Fresnel approximation, neglecting the amplitude and phase factors, which are constant in the plane:

$$u_1(x_3, y_3) \sim \int_{-\infty}^{\infty} \int_{-\infty}^{\infty} \int_{-\infty}^{\infty} t(x_1, y_1) \exp i[\varphi_0(x_1, y_1) + \varphi_1(x_1, y_1)] \exp[-ik(x_1 x_2 + y_1 y_2)/l_1] \times \exp[ik(x_2^2 + y_2^2/2l_1)] \exp[-ik(x_2^2 + y_2^2/2f_1)] \times p_1(x_2, y_2) \exp i\varphi_2(x_2, y_2) \times \exp\{ik[(x_2 - x_3)^2 + (y_2 - y_3)^2]/2l_2\} dx_1 dy_1 dx_2 dy_2, \quad (1)$$

$$u_2(x_3, y_3) \sim \int_{-\infty}^{\infty} \int_{-\infty}^{\infty} \int_{-\infty}^{\infty} t(x_1 + a, y_1) \times \exp i[\varphi_0(x_1 + a, y_1) + \varphi_1(x_1, y_1)] \times \exp[-ik(x_1 x_2 + y_1 y_2)/l_1] \exp[ik(x_2^2 + y_2^2/2l_1)] \times \exp\{-ik[(x_2 + b)^2 + y_2^2/2f_1]\} p_1(x_2 + b, y_2) \times \exp i\varphi_2(x_2 + b, y_2) \exp\{ik[(x_2 - x_3)^2 + (y_2 - y_3)^2]/2l_2\} dx_1 dy_1 dx_2 dy_2, \quad (2)$$

where k is the wave number; $t(x_1, y_1)$ is the complex transmission amplitude of the mat screen and is a random function of the coordinates; $\varphi_0(x_1, y_1)$ is a deterministic phase function which characterizes the phase distortions of the illuminating wavefront due to aberrations in the optical system forming it; l_1 and l_2 are the distances between the planes (x_1, y_1) and (x_2, y_2) and (x_2, y_2) and (x_3, y_3) , respectively; and, f_1 is the focal length of the lens L_1 with generalized pupil function⁵ $p_1(x_2, y_2)\exp i\varphi_2(x_2, y_2)$, which takes into account the axial wave aberrations.

Since $(1/f_1) = (1/l_1) + (1/l_2)$, expressions (1) and (2) assume the form

$$u_1(x_3, y_3) \sim \exp[ik(x_3^2 + y_3^2/2l_1)] \times \{t(-\mu_1x_3, -\mu_1y_3)\exp i[\varphi_0(-\mu_1x_3, -\mu_1y_3) + \varphi_1(-\mu_1x_3, -\mu_1y_3)] \otimes P_1(x_3, y_3)\}, \tag{3}$$

and

$$u_2(x_3, y_3) \sim \exp[ik(x_3^2 + y_3^2/2l_2)] \times \left\{t\left(-\mu_1x_3 - \frac{l_1b}{f_1} + a, -\mu_1y_3\right) \times \exp i\left[\varphi_0\left(-\mu_1x_3 - \frac{l_1b}{f_1} + a, -\mu_1y_3\right) + \varphi_1\left(-\mu_1x_3 - \frac{l_1b}{f_1} + a, -\mu_1y_3\right)\right] \otimes \exp(ikbx_3/l_2)P_1(x_3, y_3)\right\}, \tag{4}$$

where $\mu_1=l_1/l_2$ is the scale factor of the image transformation; \otimes denotes the convolution operation; and, $P_1(x_3, y_3) =$

$$= \int_{-\infty}^{\infty} \int_{-\infty}^{\infty} p_1(x_2, y_2)\exp i\varphi_2(x_2, y_2)\exp[-ik(x_2x_3 + y_2y_3)/l_2]dx_2dy_2$$

is the Fourier transform of the generalized pupil function of the lens L_1 .

It follows from relations (3) and (4) that if the condition $a = bl_1/f_1$ is met, then the speckle fields from the first- and second- exposure holograms coincide in the hologram plane of the focused image of the mat screen reproduced by a copy of the reference wave. It also follows that the speckle field from the second- exposure hologram has a total relative tilt angle $\alpha = b/l_2$ caused, according to Ref. 6, by the displacement of the lens L_1 in its principle plane prior the second exposure. Therefore, in the hologram plane, as was indicated in Ref. 7, the interference pattern is localized, which characterizes the phase distortions of the illuminating wavefront.

Let the spatial filtration of the diffraction field be performed in the hologram plane with the help of illumination using an opaque screen p_2 (see Fig. 1) with a circular aperture, centered on the optical axis. If the condition $\varphi_1(-\mu_1x_3, -\mu_1y_3) - \varphi_1(-\mu_1x_3 - a_3 - \mu_1y_3) \leq \pi$ is

met within the limits of the aperture, then the correlating speckle fields of two exposures immediately behind the screen can be described by the expression

$$u(x_3, y_3) \sim p_2(x_3, y_3)\exp i\varphi_3(x_3, y_3) \times \exp[ik(x_3^2 + y_3^2/2l_2)]\{t(-\mu_1x_3, -\mu_1y_3) \times \exp i\varphi_0(-\mu_1x_3, -\mu_1y_3)\otimes[1 + \exp(ikbx_3/l_2)] \times P_1(x_3, y_3)\}, \tag{5}$$

where $p_2(x_3, y_3)$ is the transmission function of the opaque screen with the circular aperture;⁸ $\varphi_3(x_3, y_3)$ is a deterministic phase function which takes into account the curvature of the substrate of the photographic plate.

The complex amplitude of the diffraction field in the detection plane 4 shown in Fig. 1 can be written in the form

$$u(x_4, y_4) \sim \int_{-\infty}^{\infty} \int_{-\infty}^{\infty} u(x_3, y_3)\exp[ik(x_3^2 + y_3^2)] \times (f_2 - l_3)/2f_2^2 \exp[-ik(x_3x_4 + y_3y_4)/f_2]dx_3dy_3, \tag{6}$$

where f_2 is the focal length of the lens L_2 ; l_3 is the distance between the lens L_2 and the plane (x_4, y_4) . If the condition $1/l_2 = (f_2 - l_3)/f_2^2$ is fulfilled then upon substituting expression (5) into expression (6) we obtain

$$u(x_4, y_4) \sim \{[p_2(-\mu_2x_4, -\mu_2y_4) \times \exp i\varphi_2(-\mu_2x_4, -\mu_2y_4) + [p_1(-\mu_2x_4 + b, -\mu_2y_4) \times \exp i\varphi_2(-\mu_2x_4 + b, -\mu_2y_4) \times F[kx_4/f_2, ky_4/f_2]] \otimes P_2(x_4, y_4)], \tag{7}$$

where $\mu_2 = l_2/f_2$ is the scale factor of the image transformation;

$$F[kx_4/f_2, ky_4/f_2] = \int_{-\infty}^{\infty} \int_{-\infty}^{\infty} t(-\mu_1x_3, -\mu_1y_3) \times \exp i\varphi_0(-\mu_1x_3, -\mu_1y_3)\exp[-ik(x_3x_4 + y_3y_4)/f_2] \times dx_3dy_3; P_2(x_4, y_4) = \int_{-\infty}^{\infty} \int_{-\infty}^{\infty} p_2(x_3, y_3) \times \exp i\varphi_3(x_3, y_3) \exp[-ik(x_3x_4 + y_3y_4)/f_2] dx_3dy_3$$

are the Fourier transforms of the corresponding functions.

As follows from relation (7), the images of the pupil of the lens L_1 are observed in the (x_4, y_4) plane, and each point of the image is broadened to the speckle size, which, in turn, is determined by the width of the function $P_2(x_4, y_4)$. In addition, the diffusely coherent light fields which correspond to the filtered regions of the image of the

mat screen are superimposed within the region of overlap of the images of the pupil of the lens L_1 and identical speckles coincide. This means that the interference pattern is localized in the plane (x_4, y_4) . Consequently, if the period of oscillation of the function $\exp i\varphi_2(-\mu_2x_4, -\mu_2y_4) + \exp i\varphi_2(-\mu_2x_4 + b, -\mu_2y_4)$ exceeds the speckle size in the detection plane 4 (Fig. 1) by an order of magnitude, then, according to Ref. 9, this function can be taken outside the convolution integral in relation (7). In this case the irradiance distribution in the (x_4, y_4) plane is given by the expression

$$I(x_4, y_4) \sim \left\{ 1 + \cos[\varphi_2(-\mu_2x_4, -\mu_2y_4) - \varphi_2(-\mu_2x_4 + b, -\mu_2y_4)] \right\} |F[kx_4/f_2, ky_4/f_2] \otimes P_2(x_4, y_4)|^2, \quad (8)$$

which describes the speckle structure modulated by the interference fringes. The interference pattern has the form of a shear interferogram with fringes of infinite width, which characterizes the axial wave aberrations due to the lens L_1 .

It can be seen on the basis of relations (3) and (4) that the information on the phase distortions introduced into the light wave by the controllable lens L_1 is carried by an individual speckle in the space of the image of the mat screen. According to Refs. 3 and 4 as follows from the form of expressions (3) and (4), the amplitude phase distribution within an individual speckle close to the optical axis is the result of the diffraction of a plane wave propagating along the optical axis, since the optical system shown in Fig. 1 constructs the image by means of two successive Fourier transforms of the light field scattered by the mat screen. Therefore the spatial filtration results in the formation of an interference pattern on the optical axis. This interference pattern characterizes the axial wave aberrations due to the lens L_1 . As to the small elements of the image of the mat screen centered at the off-axis point with coordinates $(x_{30}, 0)$, the amplitude-phase distribution within an individual speckle in this region is the result of diffraction of the off-axis plane wave propagating at the angle $\beta = x_{30}/l_2$ with respect to the optical axis. Therefore the spatial filtration results in the formation of the off-axis diffraction pattern which in a combined way characterizes the on-axis and off-axis aberrations due to the lens L_1 .

As was shown in Ref. 7, in order to record the interference pattern in the minus-first diffraction order localized in the plane of the image of the mat screen which characterizes the phase distortions of the illuminating wavefront, it is necessary to perform the spatial filtration on the optical axis in the image plane of the pupil of the lens L_1 . When reproducing the hologram in the plus-first diffraction order, the interference pattern is recorded without an additional converging lens by performing the spatial filtration in the plane of the real image of the pupil of the lens L_1 .

In contrast to Refs. 1 and 2, the method proposed here allows one to obtain the shear interferograms independently of whether the image of the mat screen coincides with the hologram plane or is localized outside this plane. Figure 2 shows an optical diagram of recording of the hologram when the image of the mat screen 1 is constructed in the (x_4, y_4) plane located at a distance l behind the photographic plate 2.

In this case when the doubly exposed hologram is reproduced by a copy of the reference wave, the complex amplitudes of the fields from the first and second exposures in the image plane take the form

$$u_1(x_4, y_4) \sim \exp[ik(x_4^2 + y_4^2)/2(l_2 + l)] \times \left\{ t(-\mu_3x_4, -\mu_3y_4) \exp i[\varphi_0(-\mu_3x_4, -\mu_3y_4) + \varphi_1(-\mu_3x_4, -\mu_3y_4)] \otimes P_3(x_4, y_4) \otimes F_1(x_4, y_4) \right\}, \quad (9)$$

$$u_2(x_4, y_4) \sim \exp[ik(x_4^2 + y_4^2)/2(l_2 + l)] \times \left\{ t(-\mu_3x_4, -\mu_3y_4) \exp i[\varphi_1(-\mu_3x_4, -\mu_3y_4) + \varphi_1(-\mu_3x_4 - a, -\mu_3y_4)] \otimes \exp(ikbx_4/(l_2 + l)) \right\} \times \otimes P_3(x_4, y_4) \otimes F_1(x_4, y_4), \quad (10)$$

where l_2 is the distance between the principle plane of the lens L_1 and the photographic plate; $\mu_3 = l_1/(l_2 + l)$ is the scale factor of the image transformation;

$$P_3(x_4, y_4) = \int_{-\infty}^{\infty} \int_{-\infty}^{\infty} p_2(x_2, y_2) \exp[i\varphi_2(x_2, y_2)] \times \exp[-ik(x_2x_4 + y_2y_4)/(l_2 + l)] dx_2 dy_2,$$

$$\Phi_1(x_4, y_4) = \int_{-\infty}^{\infty} \int_{-\infty}^{\infty} \exp[i\varphi_3(x_3, y_3)] \times \exp[-ik(x_3x_4 + y_3y_4)/l] dx_3 dy_3$$

are the Fourier transforms of the corresponding functions.

Expressions (9) and (10) assume that within the domain of existence of the function $\Phi_1(x_1, y_1)$ the phase change of the spherical wave with radius of curvature $(l_2 + l)/l_2$ does not exceed π . If the spatial filtration is performed on the optical axis in the plane (x_4, y_4) with the help of the aperture diaphragm p_2 (see Fig. 2) of lens L_2 , and the diameter of the aperture diaphragm does not exceed the interference bandwidth for the interference pattern localized in the image plane of the mat screen, then the correlating speckle fields from two exposures in the plane (x_5, y_5) are given by the expressions

$$u_1(x_5, y_5) \sim \exp[ik(x_5^2 + y_5^2)/2l_3] \times \left\{ F[kx_5/l_3, ky_5/l_3] p_1(-x_5, -y_5) \times \exp i\varphi_2(-x_5, -y_5) \exp i\varphi_3(-\mu_4x_5, -\mu_4y_5) \otimes P_3(x_5, y_5) \right\}; \quad (11)$$

$$u_2(x_5, y_5) \sim \exp[ik(x_5^2 + y_5^2)/2l_3] \times \left\{ F[kx_5/l_3, ky_5/l_3] p_1(-x_5 + b, -y_5) \times \exp i\varphi_2(-x_5 + b, -y_5) \exp i\varphi_3(-\mu_4x_5, -\mu_4y_5) \otimes P_3(x_5, y_5) \right\}, \quad (12)$$

where l_3 is the distance between the planes (x_4, y_4) and (x_5, y_5) , $\mu_4 = l/l_3$ is the scale factor of the image transformation, and

$$F[kx_5/l_3, ky_5/l_3] = \int_{-\infty}^{\infty} \int_{-\infty}^{\infty} t(-\mu_3x_4, -\mu_3y_4) \times \\ \times \exp i\varphi_0(-\mu_3x_4, -\mu_3y_4) \exp[-ik(x_4x_5 + y_4y_5)/l_3] dx_4dy_4; \\ P_3(x_5, y_5) = \int_{-\infty}^{\infty} \int_{-\infty}^{\infty} p_2(x_4, y_4) \times \\ \times \exp[-ik(x_4x_5 + y_4y_5)/l_3] dx_4dy_4$$

are the Fourier transforms of the corresponding functions.

In order to simplify the formulas, expressions (11) and (12) are written assuming that lens 2 in Fig. 2 forms an image of the pupil of lens L_1 in the plane (x_5, y_5) at unit magnification. Based on these expressions, we obtain the following irradiance distribution in the recording plane 4:

$$I(x_5, y_5) \sim \{1 + \cos[\varphi_2(-x_5 + b, -y_5) - \\ - \varphi_2(-x_5, -y_5)]\} |F[kx_5/l_3, ky_5/l_3] \times \\ \times \exp i\varphi_3(-\mu_4x_5, -\mu_4y_5) \otimes P_3(x_5, y_5)|^2. \quad (13)$$

It follows from relation (13) that the shear interference pattern in fringes of infinite width modulates the speckle structure. The distortions introduced in the light wave due to the curvature of the substrates of the mat screen and the photographic plate are localized within a speckle and do not alter the interference pattern characterizing the axial wave aberrations due to the lens L_1 .

In order to extend the range of control of a lens or an objective over the field angle (for fixed spatial resolution of the medium in which the hologram is recorded), let us consider the recording of a double-exposure hologram of the focused image of the mat screen 1 in Fig. 3a by a divergent spherical reference wave. If the curvature radius of this wave in the plane of the photographic plate 2 is equal to the distance between the plate and the principal plane of the lens L_1 , then the width of the spatial frequency spectrum of the hologram of the focused image in the directions of the coordinate axes is determined only by the angular dimensions of the illuminated zone of the mat screen taking into account the scale factor of the transformation and displacement of the point source S of the reference wave with respect to the center of the mat screen.

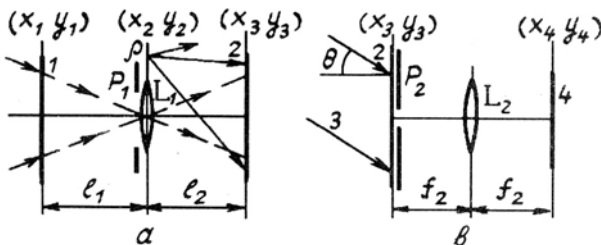


FIG. 3. Optical diagram of recording (a) and reconstruction (b) of the double-exposure hologram of the focused image produced by a divergent spherical reference wave.

If the hologram 2 in Fig. 3b is reproduced by a plane wave incident at an angle c/l_2 , where c is x -coordinate of the center of the spherical reference wave, the diffraction field in the hologram plane takes the form

$$u(x_3, y_3) \sim \{ \{ t(-\mu_1x_3, -\mu_1y_3) \exp i[\varphi_0(-\mu_1x_3, -\mu_1y_3) + \\ + \varphi_1(-\mu_1x_3, -\mu_1y_3)] \otimes P_1(x_3, y_3) \} + \{ t(-\mu_1x_3, -\mu_1y_3) \times \\ \times \exp i[\varphi_0(-\mu_1x_3, -\mu_1y_3) + \varphi_1(-\mu_1x_3 - a, -\mu_1y_3)] \} \otimes \\ \otimes \exp(ikbx_3/l_2) P_1(x_3, y_3) \} \} \exp i\varphi_3(x_3, y_3). \quad (14)$$

From Eq. (14) it follows that the speckle fields from both exposures coincide in the hologram plane in which the interference pattern characterizing the phase distortions of the illuminating wavefront is localized. In addition, it is seen that the interference pattern characterizing the wave aberrations due to the lens L_1 is localized in the far diffraction zone since the factor in Eqs. (3) and (4) describing the phase distribution of the divergent spherical wave with radius of curvature l_2 in the hologram plane is absent in Eq. (14). This interference pattern should be recorded in the focal plane of lens 2 (Fig. 3b) when performing the spatial filtration in the hologram plane with the help of the diaphragm p_2 .

Assuming that lens the L_1 introduces vignetting^{1,2} during the recording of the hologram produced by the divergent spherical reference wave, we shall consider in more detail the recording of the interference pattern localized in the hologram plane.

If we assume that the diameter of the lens L_2 (Fig. 4a) is greater than that of the image of the mat screen in the hologram plane 2, then the light field in the back focal plane (x_4, y_4) of the lens 2 can be represented as a Fourier transform

$$u(kx_4/f_2, ky_4/f_2) = F[u(x_3, y_3)], \quad (15)$$

where F denotes the Fourier transform.

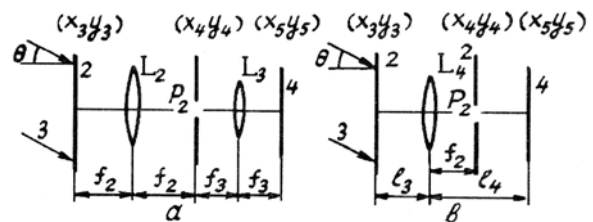


FIG. 4. Optical diagram of the recording of the interference pattern localized in the hologram plane of the focused image formed with the help of the collimating system of the lenses L_2 and L_3 (a) and the single lens L_4 (b).

Let an opaque screen p_2 with a circular aperture centered on the optical axis be positioned in the plane (x_4, y_4) . If the diameter of the filtering aperture does not exceed the interference bandwidth of the interference pattern localized in the far diffraction zone, then on the basis of Eqs. (14) and (15), the light field at the exit from the filtering aperture takes the form

$$u(x_4, y_4) \sim p_2(x_4, y_4) \left\{ \left\{ F_1[kx_4/f_2, ky_4/f_2] + F_2[kx_4/f_2, ky_4/f_2] \right\} \otimes \Phi_2(x_4, y_4) \right\}, \quad (16)$$

where

$$F_1[kx_4/f_2, ky_4/f_2] = \int_{-\infty}^{\infty} \int_{-\infty}^{\infty} t(-\mu_1 x_3, -\mu_1 y_3) \times \exp i[\varphi_0(-\mu_1 x_3, -\mu_1 y_3) + \varphi_1(-\mu_1 x_3, -\mu_1 y_3)] \times \exp[-ik(x_3 x_4 + y_3 y_4)/f_2] dx_3 dy_3;$$

$$F_2[kx_4/f_2, ky_4/f_2] = \int_{-\infty}^{\infty} \int_{-\infty}^{\infty} t(-\mu_1 x_3, -\mu_1 y_3) \exp i[\varphi_0(-\mu_1 x_3, -\mu_1 y_3) + \varphi_1(-\mu_1 x_3 - a, -\mu_1 y_3)] \exp[-ik(x_3 x_4 + y_3 y_4)/f_2] dx_3 dy_3;$$

$$\Phi_2(x_4, y_4) = \int_{-\infty}^{\infty} \int_{-\infty}^{\infty} \exp i\varphi_3(x_3, y_3) \exp[-ik(x_3 x_4 + y_3 y_4)/f_2] dx_3 dy_3$$

are the Fourier transforms of the corresponding functions.

The lens L_3 (Fig. 4a) with focal length f_3 realizes the Fourier transform of the filtered-out field, thus forming in its back focal plane the distribution

$$u(x_5, y_5) \sim \left\{ \exp i\varphi_1(\mu_1 \mu_5 x_5, \mu_1 \mu_5 y_5) + \exp i\varphi_1(\mu_1 \mu_5 x_5 - a, \mu_1 \mu_5 y_5) \right\} \times \left\{ t(\mu_1 \mu_5 x_5, \mu_1 \mu_5 y_5) \exp i[\varphi_0(\mu_1 \mu_5 x_5, \mu_1 \mu_5 y_5) + \varphi_3(-\mu_5 x_5, -\mu_5 y_5)] \right\} \otimes P_4(x_5, y_5), \quad (17)$$

where $\mu_3 = f_2/f_3$ is the scale factor of the image transformation;

$$P_4(x_5, y_5) = \int_{-\infty}^{\infty} \int_{-\infty}^{\infty} p_2(x_4, y_4) \exp[-ik(x_4 x_5 + y_4 y_5)/f_3] dx_4 dy_4$$

is the Fourier transform of the transmission function of the filtering screen.

As follows from Eq. (17), the correlating speckle fields from two exposures coincide in the recording plane 4 (Fig. 4a), and if the period of variation of function $\exp i\varphi_1(\mu_1 \mu_5 x_5, \mu_1 \mu_5 y_5) + \exp i\varphi_1(\mu_1 \mu_5 x_5 - a, \mu_1 \mu_5 y_5)$ exceeds the speckle size, which is determined by the width of the function $P_4(x_5, y_5)$, then the irradiance distribution in the recording plane is given by

$$I(x_5, y_5) \sim \left\{ 1 + \cos[\varphi_1(\mu_1 \mu_5 x_5, \mu_1 \mu_5 y_5) - \varphi_1(\mu_1 \mu_5 x_5 - a, \mu_1 \mu_5 y_5)] \right\} \left| t(\mu_1 \mu_5 x_5, \mu_1 \mu_5 y_5) \times \exp i[\varphi_0(\mu_1 \mu_5 x_5, \mu_1 \mu_5 y_5) + \varphi_3(-\mu_5 x_5, -\mu_5 y_5)] \otimes P_4(x_5, y_5) \right|^2. \quad (18)$$

Expression (18) describes the speckle structure modulated by the interference fringes. The interference pattern in this case is the shear interferogram in fringes of infinite width, and characterizes the phase distortions of the illuminating wavefront.

The spatial filtration of the light field on the optical axis in the far diffraction zone following the optical scheme shown in Fig. 4b results in the following distribution of the light field at the exit from the filtering aperture p_2 :

$$u(x_4, y_4) \sim p_2(x_4, y_4) \exp[ik(x_4^2 + y_4^2)] \times (f_2 - l_3)/2f_2^2 \left\{ \left\{ F_3[kx_4/f_2, ky_4/f_2] + F_4[kx_4/f_2, ky_4/f_2] \right\} \otimes \Phi_2(x_4, y_4) \right\}, \quad (19)$$

where l_3 is the distance between the hologram and the lens L_2 ; and,

$$F_3[kx_4/f_2, ky_4/f_2] = \int_{-\infty}^{\infty} \int_{-\infty}^{\infty} p_1(x_3, y_3) \times t(-\mu_1 x_3, -\mu_1 y_3) \exp i[\varphi_0(-\mu_1 x_3, -\mu_1 y_3) + \varphi_1(-\mu_1 x_3, -\mu_1 y_3)] \exp[-ik(x_3 x_4 + y_3 y_4)/f_2] dx_3 dy_3;$$

$$F_4[kx_4/f_2, ky_4/f_2] = \int_{-\infty}^{\infty} \int_{-\infty}^{\infty} p_1(x_3, y_3) \times t(-\mu_1 x_3, -\mu_1 y_3) \exp i[\varphi_0(-\mu_1 x_3, -\mu_1 y_3) + \varphi_1(-\mu_1 x_3 - a, -\mu_1 y_3)] \exp[-ik(x_3 x_4 + y_3 y_4)/f_2] dx_3 dy_3$$

are the Fourier transforms of the corresponding functions.

Expression (19) takes into account the fact that the lens L_1 transforms the light information on the mat screen which is carried by the components with spatial frequencies up to $\nu_{max} = d/2\lambda l_1$ into the image, where d is the diameter of the lens L_1 , and λ is the radiation wavelength of the coherent light source which is used to record and to reproduce the hologram. Assuming that lens L_2 re-forms the image of the mat screen in the plane (x_5, y_5) , i.e., $(1/f_2) = (1/l_3) + (1/l_4)$, we obtain the distribution of the diffraction field in the recording plane 4 in the form

$$u(x_5, y_5) \sim \exp[ik(x_5^2 + y_5^2)/2(l_4 - f_2)] \times \left\{ p_1(-\mu_6 x_5, -\mu_6 y_5) t(\mu_1 \mu_6 x_5, \mu_1 \mu_6 y_5) \times \exp i[\varphi_0(\mu_1 \mu_6 x_5, \mu_1 \mu_6 y_5) + \varphi_3(-\mu_6 x_5, -\mu_6 y_5)] \right\} \times \left\{ \exp i\varphi_1(\mu_1 \mu_6 x_5, \mu_1 \mu_6 y_5) + \exp i\varphi_1(\mu_1 \mu_6 x_5 - a, \mu_1 \mu_6 y_5) \right\} \otimes P_5(x_5, y_5), \quad (20)$$

where $\mu_6 = l_3/l_4$ is the scale factor of the image re-formation; and,

$$P_5(x_5, y_5) = \int_{-\infty}^{\infty} \int_{-\infty}^{\infty} p_2(x_4, y_4) \exp[-ik(x_4x_5 + y_4y_5)/(l_4 - f_2)] dx_4 dy_4$$

is the Fourier transform of the transmission function of the filtering screen.

On the basis of relation (20), the superposition of the correlating speckle fields results in the following irradiance distribution:

$$I(x_5, y_5) \sim \{1 + \cos[\varphi_1(\mu_1\mu_6x_5, \mu_1\mu_6y_5) - \varphi_1(\mu_1\mu_5x_5 - a, \mu_1\mu_5y_5)]\} |p_1(-\mu_6x_5, -\mu_6y_5) \times \ell(\mu_1\mu_6x_5, \mu_1\mu_6y_5) \exp i[\varphi_0(\mu_1\mu_6x_5, \mu_1\mu_6y_5) + \varphi_3(-\mu_6x_5, -\mu_6y_5)]| \otimes |P_5(x_5, y_5)|^2. \tag{21}$$

In this case, the dimensions of the interference pattern characterizing the phase distortions of the illuminating wavefront is limited by the diameter of the aperture diaphragm of the lens L_1 .

In our experiment we recorded the double-exposure holograms on Mikrat-VRL photographic plates using a He-Ne laser with wavelength $\lambda = 0.63 \mu\text{m}$. Figure 5a shows an example of a shear interferogram formed when the photographic plate is displaced by the distance $b = 1 \text{ mm}$, with spatial filtration on the optical axis in the image plane of the mat screen.

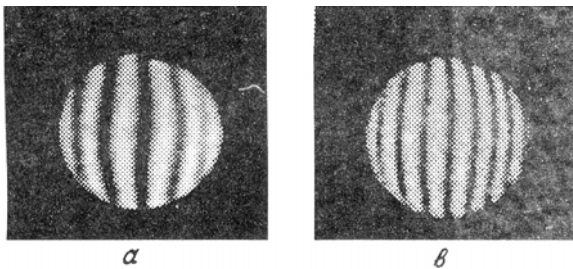


FIG. 5. Shear interferograms recorded when performing the spatial filtration in the image plane (a) and in the hologram plane (b).

The interference pattern characterizes the spherical aberration due to the lens L_1 with focal length $f_1 = 160 \text{ mm}$ and diameter $d = 24 \text{ mm}$ with prefocal defocusing, which forms the hologram of the focused image at unit magnification localized at a distance $l = 100 \text{ mm}$ from the photographic plate. Spatial filtration of the double-exposure hologram recorded in this way in its plane on the optical axis yields an interference pattern with a greater number of interference fringes (Fig. 5b). The change in the number of interference fringes is explained by the fact that when performing filtration in the image plane, the effect of the phase distortions of the illuminating wavefront is completely excluded. With the filtering aperture is removed from the image plane the spatial frequency of the interference fringes, which reflect the phase distortions of illuminating wavefront, increase, and the contribution of the wave aberrations due to the lens L_1 to the interference pattern decreases.

Figure 6a shows the shear interferogram recorded in the far diffraction zone when performing the spatial filtration on the optical axis in the hologram plane and reproduced by a laser beam with diameter 1 mm. The double-exposure hologram of the image of the mat screen focused on the photographic plate at unit magnification was recorded by the divergent spherical reference wave. The values of displacements were $a = 2 \text{ mm}$ and $b = 1 \text{ mm}$ with an accuracy not worse than 0.002 mm. The focal length of the lens L_1 was equal to 180 mm, the distance d was equal to 20 mm, and the diameter of the illuminated spot on the mat screen was 45 mm. The interference pattern characterizes the spherical aberration due to the lens L_1 at the paraxial focus. Performing spatial filtration on the x axis parallel to the displacement at the point $x_{30} = 14 \text{ mm}$, $y_{30} = 0$ results in the formation of the interference pattern shown in Fig. 6b which represents a combination of the on-axis wave aberrations shown in Fig. 6a and off-axis aberrations of the coma type. The interference pattern localized in the hologram plane is shown in Fig. 6c.

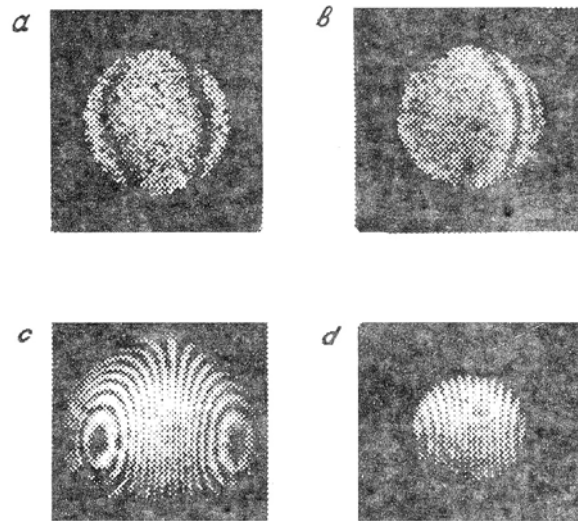


FIG. 6. Shear interferograms recorded when performing on-axis spatial filtration in the hologram plane (a), off-axis spatial filtration in the hologram plane (b), in the frequency domain with the help of the collimating system of lenses (c), and with a single lens (d).

This shear interferogram characterizes the spherical aberration with postfocal defocusing of the wave illuminating the mat screen. The interferogram was recorded with the help of a collimating system of lenses with the spatial filtration performed on the optical axis in the frequency domain with the help of a filtering aperture 5 mm in diameter. When the hologram is reconstructed according to Fig. 4b, the interference pattern is limited by the aperture of the lens L_1 , as shown in Fig. 6d. It should be noted that when reconstructing the hologram in the plus first diffraction order, the interference pattern characterizing the wave aberrations due the lens L_1 is also localized in the far diffraction zone while the interference pattern produced as a result of the phase distortions of the illuminating wavefront is localized in the hologram plane. The hologram, in its turn, is recorded with the help of the collimating system of lenses. When it is recorded with the single lens, the field of view is also limited by the aperture of the lens L_1 .

The results obtained here demonstrate the following salient features of holographic differential interferometry based on the use of diffusely scattered light fields. The interference pattern characterizing the wave aberrations due to the lens used to record the double-exposure hologram of the focused image of the mat screen and the interference pattern characterizing the distortions of the illuminating wavefront are localized in different planes. This makes it possible to record them independently when performing spatial filtration. The phase distortions introduced into the light wave by the curvature of the mat screen and the photographic plate are localized within a speckle and do not influence the interference pattern.

REFERENCES

1. V.G. Gusev, *Atm. Opt.* **3**, No. 9, 857–865 (1990).
2. V.G. Gusev, *Atm. Opt.* **3**, No. 10, 947–955 (1990).
3. R. Kollier, K. Burkhart, and L. Leen, *Optical Holography* [Russian translation] (Moscow, Mir, 1973), 670 pp.
4. S.M. Gorskii, V.A. Zverev, and A.L. Matveev, *Izv. Vyssh. Uchebn. Zaved. Ser. Radiofiz.* **20**, No. 4, 522–527 (1977).
5. J. Goodman, *Introduction into Fourier Optics* [McGraw Hill, New York, 1968].
6. V.G. Gusev and S.V. Lazarev, *Opt. Mekh. Prom.*, No. 9, 8–10 (1986).
7. V.G. Gusev, *Izv. Vyssh. Uchebn. Zaved. Ser. Priborostroenie* **32**, No. 5, 65–70 (1989).
8. M. Born and E. Wolf, *Principles of Optics*, 4 th ed. Pergamon Press, Oxford' (1970).
9. R. Jones and K. Wikes, *Holographic and Speckle Interferometry* [Russian translation] (Moscow, Mir, 1986), 320 pp.